PHYSICAL REVIEW D **87,** 043508 (2013)

Moduli dark matter and the search for its decay line using Suzaku x-ray telescope

Alexander Kusenko,[1,2] Michael Loewenstein,[3,4] and Tsutomu T. Yanagida[2]

[1]*Department of Physics and Astronomy, University of California, Los Angeles, California 90095-1547, USA*
[2]*Kavli Institute for the Physics and Mathematics of the Universe, University of Tokyo, Kashiwa, Chiba 277-8568, Japan*
[3]*Department of Astronomy, University of Maryland, College Park, Maryland 20742, USA*
[4]*CRESST and X-ray Astrophysics Laboratory NASA/GSFC, Greenbelt, Maryland 20770, USA*

(Received 27 September 2012; published 4 February 2013)

Light scalar fields called moduli arise from a variety of different models involving supersymmetry and/or string theory; thus their existence is a generic prediction of leading theories for physics beyond the standard model. They also present a formidable, long-standing problem for cosmology. We argue that an anthropic solution to the moduli problem exists in the case of small moduli masses and that it automatically leads to dark matter in the form of moduli. The recent discovery of the 125 GeV Higgs boson implies a lower bound on the moduli mass of about a keV. This form of dark matter is consistent with the observed properties of structure formation, and it is amenable to detection with the help of x-ray telescopes. We present the results of a search for such dark matter particles using spectra extracted from the first deep x-ray observations of the Draco and Ursa Minor dwarf spheroidal galaxies, which are dark-matter-dominated systems with extreme mass-to-light ratios and low intrinsic backgrounds. No emission line is positively detected, and we set new constraints on the relevant new physics.

DOI: 10.1103/PhysRevD.87.043508 PACS numbers: 95.35.+d, 12.60.Jv

I. THE NATURE AND ORIGIN OF MODULI

Superstring theories, widely considered as candidates for a unified theory of all interactions, generically predict the existence of light scalar fields associated with the breaking of scale invariance and the size and shape of the string compactification volume. One example is the dilaton, a scalar field associated with the scale transformations whose vacuum expectation value (VEV) determines the values of various couplings in the low-energy effective field theory. String theory compactification radii also appear in the low-energy theory as scalar fields with some very small masses. In a number of models, the string scale M_s is of the order of the reduced Planck mass, $M_{\rm G} = M_{\rm P}/\sqrt{8\pi} = 2.4 \times 10^{18}$ GeV, but, in models with a large compactification volume, the scale of M_s is suppressed by the compactification volume and can be much lower [1]. Although one might expect that interactions of moduli with other fields should be suppressed by a factor that is proportional to some power of $M_{\rm G}$, detailed calculations can produce answers that are different from naive dimensional analyses [2].

Supersymmetry is a generic prediction of string theory, but, even aside from string theory, it is a well-motivated concept in its own right. An appealing generalization of space-time symmetries involving noncommuting fermionic degrees of freedom in the form of a graded algebra leads to supersymmetry and supersymmetric extensions of the standard model. As long as supersymmetry is unbroken, its potential has numerous flat directions with infinitely many degenerate classical vacua. The degrees of freedom parametrizing these flat directions are massless in the limit of unbroken supersymmetry, but they acquire a mass from the breaking of supersymmetry. The mass thus acquired is well below the scale at which supersymmetry breaking occurs. For example, for F-type breaking, the breaking of supersymmetry by the nonzero VEV of $|F|$ can be communicated to the rest of the fields by gravitational interactions suppressed by the (reduced) Planck mass $M_{\rm G}$. This gives moduli masses of the order of $m \sim |F|/M_{\rm G}$, well below the scale of supersymmetry breaking. The coupling of the moduli to the rest of the fields is also suppressed by the higher scale.

II. THE MODULI MASSES

Massless in the limit of exact supersymmetry, the moduli acquire some masses from supersymmetry breaking. The range of moduli masses is model dependent, and a lighter scalar with mass well below a keV would not be a viable dark matter candidate. However, the recent discovery of a 125 GeV Higgs boson [3,4] points to the moduli masses above 1 keV, which further strengthens the motivation for investigating moduli as a viable dark matter candidate.

In the following section we directly address the moduli problem, and our approach is based on a low-scale supersymmetry breaking. Therefore, we consider the gauge-mediated supersymmetry breaking scenario. The breaking of supersymmetry occurs via a nonzero vacuum expectation value (VEV) of the F component $\langle F_S \rangle \neq 0$ of some chiral superfield S, whose scalar component also has a nonzero VEV $\langle S \rangle$. Supersymmetry breaking is then communicated to the visible sector by messengers Ψ_i. The messengers couple to S with couplings λ_{ij},

$$W = \lambda_{ij} S \Psi_i \bar{\Psi}_j. \tag{1}$$

In what follows we suppress the indices as we discuss the generic features of a class of models. The mass-squared matrix of the scalar messengers takes the form

$$\begin{pmatrix} |\lambda\langle S\rangle|^2 & \lambda\langle F_S\rangle^\dagger \\ \lambda\langle F_S\rangle & |\lambda\langle S\rangle|^2 \end{pmatrix}. \quad (2)$$

The stability condition requires that this matrix have no negative eigenvalues, which implies

$$M^2_{\rm mess} \equiv |\lambda\langle S\rangle|^2 \geq |\lambda\langle F_S\rangle|. \quad (3)$$

In the visible sector, the squarks acquire masses through the gauge interactions involving the messengers in the loops. Up to some group theoretical factors of order one, these masses are

$$m_{\rm sq} \simeq \frac{\alpha_3}{4\pi}\frac{\lambda\langle F_S\rangle}{M_{\rm mess}}, \quad (4)$$

where α_3 is the SU(3) gauge coupling constant of quantum chromodynamics (QCD). The recent discovery of the Higgs boson with mass 125 GeV significantly tightens the allowed range of parameters for the squark masses. According to the analysis of Refs. [5,6], a mass of 125 GeV requires that the squarks be heavier than 10 TeV. The constraint

$$m_{\rm sq} > 10 \text{ TeV}, \quad (5)$$

combined with Eq. (4), the stability constraint Eq. (3), and the requirement that $\lambda < 1$ implies the following lower limit on the supersymmetry breaking scale $|F| \equiv |F_S| + (\text{other contributions}) > |F_S|$,

$$|F| \geq |F_S| > \left(\frac{m_{\rm sq}}{10 \text{ TeV}}\right)^2 (10^6 \text{ GeV})^2. \quad (6)$$

We note that $|F| = |F_S|$ in the case of direct mediation [7].

This lower bound on the supersymmetry breaking scale implies the following lower bound on the mass of the moduli:

$$m_\phi = \frac{|F|}{M_{\rm G}} > 1 \text{ keV}. \quad (7)$$

Some moduli can get larger masses, for example, if they couple directly to the gauge fields in the hidden sector, where gaugino condensation takes place. However, it is likely that some moduli remain massless until supersymmetry is broken and get masses of the order of the gravitino mass in Eq. (7) by gravity mediation. We will focus on such moduli.

Some additional constraints arise from the requirement of not overproducing dark matter in the form of gravitinos, which have a similar mass. For masses in the several keV range, the gravitinos come into thermal equilibrium and reach thermal abundances at temperatures above TeV, and the total amount of dark matter would be unacceptably large if no dilution occurred. However, gauge-mediated supersymmetry breaking models contain candidate particles whose out-of-equilibrium decay can produce entropy and dilute the population of dark matter to an acceptable level [8,9]. The required dilution factor Δ is proportional to the mass, $\Delta \sim 100(m_{3/2}/10 \text{ keV})$ [8]. For masses above 1 MeV, the requisite dilution of $\Delta \sim 10^4$ can be difficult to reconcile with leptogenesis because the baryon asymmetry is diluted by the same factor. For masses below (but not too far below) 1 MeV, the dilution can still be efficient and the gravitino abundance, well below the observed dark matter abundance. As we discuss below, the moduli generally tend to be overproduced, but anthropic selection considerations point to abundances in the range of observational estimates of the dark matter density. Since the same anthropic reasoning would not work for the gravitinos, one can assume that the moduli have a greater abundance than the gravitinos. It is also possible that the contributions of the moduli and the gravitinos are comparable. The intriguing possibility that dark matter is composed of two separate components with different free-streaming properties, which can have some observable effects on the small scales, was discussed in detail [10–12] in connection with sterile neutrinos produced by two distinct mechanisms [10,13–16]. In our case, there is an analogous possibility that dark matter is comprised of two components, namely, the moduli and the gravitinos.

Taking into account the Higgs boson mass and the gravitino constraints, the moduli masses of interest lie in the range $m_\phi \simeq (1\text{–}10^3)$ keV.

III. THE MODULI PROBLEM

As discussed above, a number of independent arguments based on well-motivated theories converge on the prediction of light scalar fields coupled very weakly to the remaining fields in the theory. The relevant masses range from a few eV to well above the electroweak scale. The lighter moduli can decay through interactions suppressed by an effective high-energy scale $\Lambda_{\rm eff}$ into photons and neutrinos. Typically, the dominant decay channel is $\phi \to \gamma\gamma$ through a coupling

$$\mathcal{L}_{\rm int} = \frac{1}{4\Lambda_{\rm eff}}\phi F_{\mu\nu}F^{\mu\nu} = \frac{b}{4M_{\rm G}}\phi F_{\mu\nu}F^{\mu\nu}, \quad (8)$$

where we have defined a parameter b,

$$b = \frac{M_{\rm G}}{\Lambda_{\rm eff}}, \quad (9)$$

choosing b and $\Lambda_{\rm eff}$ so as to parametrize the coupling in a model-independent way. $\Lambda_{\rm eff}$ and the corresponding parameter b have specific meanings in the context of specific models. For example, for string moduli, $\Lambda_{\rm eff}$ can be related to the string compactification scale and structure. Explicit calculations yield values of b ranging from $b = \sqrt{2} \sim 1$ [17] to much larger values [2].

The rate of moduli radiative decay is

$$\Gamma_{\phi\to\gamma\gamma} = b^2 \frac{m_\phi^3}{64\pi M_{\rm G}^2}. \quad (10)$$

The generic prediction of light scalar fields gives rise to a very serious cosmological problem, namely the moduli problem. There is strong and growing evidence that the Universe has undergone a period of inflation that resulted in flatness and homogeneity of the observed Universe and that generated the observed spectrum of density perturbations. If mass m_ϕ is smaller than the Hubble constant H during inflation, then the vacuum expectation value of the light scalar field during inflation can be very large for the following reason. One expects the energy density in each scalar field to be of the order of H^4, that is $m^2\phi^2 \sim H^4$, during inflation. Hence, the VEV $\langle\phi\rangle$, on average (i.e., averaged over superhorizon scales), takes a very large value. Furthermore, the value of the ground-state VEV is not well defined. During inflation, the minimum of the potential for the ϕ field can differ from its zero-temperature value due to the terms associated with supersymmetry breaking in de Sitter space, i.e., due to expansion of the Universe. These terms, coming from the Kähler potential, act as additional mass terms $cH^2\phi^2$, where c is a constant of order 1 that can be positive or negative [18,19]. These contributions overwhelm the small moduli masses and can displace the VEV of the field by a large amount. When inflation is finished, and reheating commences, the VEVs of the moduli fields are stuck at some values far from the minima of their respective potentials. Eventually the Hubble constant H approaches the mass m_ϕ, and only then can the field start oscillating. However, the minimum of the effective potential, which includes the expansion-induced contributions, can still differ from the zero temperature minimum.[1]

A scalar field with some vanishingly small couplings to the lighter particles oscillates until the time

$$\tau_{\phi\to\gamma\gamma} = \Gamma^{-1}_{\phi\to\gamma\gamma} = 7.6\times 10^{32}\left(\frac{1}{b}\right)^2\left(\frac{1\ {\rm keV}}{m_\phi}\right)^3\ {\rm s}. \quad (11)$$

During this time, the field's cosmological behavior is identical to that of nonrelativistic matter, with energy density declining with scale factor a as $1/a^3$. When the radiation density that scales as $1/a^4$ drops below the energy density of moduli, the Universe enters a prolonged period of matter-dominated expansion, at the end of which moduli decay. This causes a variety of cosmological problems, depending on the moduli mass and decay width.

[1]This stymies some of the attempted solutions: even if the moduli oscillations can be damped at some point in the expanding Universe for some specific value of the Hubble parameter H, they are bound to resume when H decreases further because the minimum of the effective potential depends on H [19].

If moduli decay before big-bang nucleosynthesis, their decay products thermalize and they do not cause a conflict with observations, assuming that the baryon asymmetry of the Universe is not diluted away. It is possible to generate the baryon asymmetry through Affleck-Dine baryogenesis [20–22] so as to compensate for dilution. Masses m_ϕ above 10^2 TeV may be considered "safe" in this sense. If the moduli decay during big-bang nucleosynthesis, the entropy release may still be consistent with successful nucleosynthesis, and the additional entropy released may account for the small observed deviation of the effective number of light species from the standard model prediction [23,24]. This case requires further investigation.

Moduli decay after nucleosynthesis, but before recombination, unacceptably dilutes the baryon density. Decay after recombination also distorts the cosmic diffuse microwave, and contributes to the x- and gamma-ray, backgrounds in violation of observational constraints for some combinations of abundance and mass [25–27], although cosmologically significant densities are not excluded for $m_\phi < 100$ keV [28].

Finally, although decay times longer than the age of the Universe are consistent with the moduli being the dark matter if they can be produced with the correct abundance, naive estimates for moduli dark matter abundance in this case predict a much greater value than the observed dark matter density. Indeed, let us estimate the energy density of the Universe when the modulus ϕ starts oscillating, that is when $H \sim m_\phi$, or when the temperature of the Universe is

$$T_\phi \sim (90/\pi^2 g_*)^{1/4}\sqrt{M_{\rm G} m_\phi}. \quad (12)$$

The density-to-entropy ratio is

$$\frac{\rho_\phi}{s} \sim \frac{m_\phi^2\phi_0^2/2}{(2\pi^2/45)g_* T_\phi^3} \sim 10^5\ {\rm GeV}\left(\frac{m_\phi}{\rm keV}\right)^{1/2}\left(\frac{\phi_0}{M_{\rm G}}\right)^2. \quad (13)$$

Comparing this ratio, corrected for the entropy production, with today's value,

$$\frac{\rho_{\rm DM}}{s} = 0.2\frac{\rho_c}{s} = 3\times 10^{-10}\ {\rm GeV}, \quad (14)$$

clearly reveals a drastic discrepancy.

With the help of thermal inflation [29,30], or by means of coupling the moduli fields to the inflaton [31,32], the moduli problem can be ameliorated in some range of masses [25–27]. However, neither of these approaches provides a complete solution.

IV. ANTHROPIC SELECTION

As long as the moduli are long lived, anthropic selection may be invoked to explain why moduli dark matter in the observed part of the Universe is present in the right amount, circumventing the problem discussed in the previous section of the energy density in the oscillating moduli field taking on an excessively large value. The moduli

problem is eliminated if the initial value ϕ_0 of the modulus field is, for whatever reason, sufficiently small that the energy density in the moduli does not significantly exceed the baryonic energy density. This may be compared with the requirement, realized in the observable Universe, for the dark-to-baryonic matter ratio to be ~ 4 in order for conditions amenable to the the formation of stars and planets and, ultimately, for the existence of life to be attained [33]. Therefore, one may simultaneously attempt to explain away the moduli problem and explain the abundance of dark matter based on the anthropic selection: life can only emerge in those parts of the Universe where the moduli energy density is sufficiently low that the dark-to-baryonic matter ratio has the acceptable value.

The reasoning here is analogous to that applied to the axion [34]. Indeed, the abundance of string moduli depends on the initial value ϕ_0 [Eq. (13)] that is determined by the VEV of the field during inflation. On average, this VEV tends to be very large, of the order of $M_{\rm G}$. However the large VEV may generate too much matter that is already dominant at a temperature $T \sim 10^5$ GeV. Inflation still assures that $\Omega = 1$, so that the Universe remains flat; however, in this case, structure formation proceeds very early, leading to a universe dominated by black holes [33,35]. If matter comes to dominate the energy density of the Universe too early, the density perturbations can grow and become nonlinear before recombination. In this case, baryons and radiation are trapped together inside the collapsing halos, and the baryon coupling to photons maintains the Jeans mass at a constant value as the collapse proceeds. As a result, the baryonic matter cannot fragment, and large amounts of coupled baryon-radiation fluid are dragged into the potential wells created by clumps of dark matter. As discussed by Ref. [33], the end result of such a structure formation process is a universe with supermassive black holes, photons, and neutrinos, but without stars and planets. Such a universe is not amenable to life. For the example in question, the matter-radiation equality would occur at temperature

$$T_{\rm eq} \sim 10^5 \text{ GeV} \left(\frac{m_\phi}{\text{keV}}\right)^{1/2} \left(\frac{\phi_0}{M_{\rm G}}\right)^2. \quad (15)$$

Assuming that the baryon asymmetry escapes dilution, baryons are coupled to radiation until $T_{\rm rec} \sim 1$ eV. Linear growth of density perturbations may commence as early as at redshift $z \sim 10^{13}$, allowing for a longer epoch of growth in cosmological perturbations. In the observed Universe, primordial perturbations of the order of $\delta\rho/\rho \sim 10^{-5}$ are consistent with the data. However, in the Universe with matter domination starting as early as redshift $z \sim 10^{13}$, these perturbations would have gone nonlinear long before recombination, leading to a universe dominated by black holes and not stars and planets capable of hosting life. In fact, even the overdensities as small as 10^{-9} would have gone nonlinear in this case. The possibility of starting with very small density perturbations $Q \equiv \delta\rho/\rho < 10^{-8}$ is disfavored by some anthropic arguments as well. The constraints arise from a combination of several astrophysical bounds summarized in Table 4 and Fig. 12 of Ref. [33], which show the anthropically allowed range as a function of Q and matter density per cosmic microwave background photon. There one finds no viable possibility for $Q < 10^{-8}$ and any matter density. Likewise, there is no viable scenario for any value of Q for large dark matter densities.

We conclude that life is impossible in a universe where the dark matter density exceeds the baryon density by many orders of magnitude, and we refer the reader to Refs. [33,35] for a detailed discussion.

While the ''most common'' values of the initial field ϕ produce universes without stars or planets, inflation does allow for some relatively small part of the volume to have $\phi_0 \ll M_{\rm G}$. The probability of this happening at any given point in de Sitter space is negligible, but the conditional probability of a small VEV, under the condition that life can evolve and produce an observer, is actually of the order of 1 because life is highly improbable in the large-VEV regions. Hence, anthropic selection would favor $\phi_0 \sim 10^{-8} M_{\rm G}$, near the boundary of the parameter space acceptable for the existence of life.

This motivates the search for dark matter in the form of string moduli with masses below 1 MeV and for decay widths corresponding to $b = 1$–10^3. Cosmological data limits the lifetime of dark matter to $\tau_{\phi\to\gamma\gamma} > 10^{24}$ s in the case of radiative decays [36,37] (and $\tau_{\phi\to\gamma\gamma} > 3 \times 10^{18}$ s for general decays [37]). Based on Eq. (11), this corresponds to sub-MeV masses. In particular, one can search for the dark matter in the form of moduli using x-ray telescopes.

V. SEARCH FOR MODULI DARK MATTER IN X-RAYS

The decay of moduli into two photons presents an opportunity for a possible discovery using x-ray telescopes. Since this is a two-body decay, the signal is a very narrow line, whose width is determined by the Doppler broadening due to the motion of the dark matter particles. The energy of a photon is $(1/2)$ of the particle mass.

If such a line is detected by the x-ray telescopes from compact astrophysical objects with substantial dark mater content and/or from diffuse radiation due to the galactic and cosmological distributions of dark matter, the wavelength of the line will provide a measurement of the dark-matter particle mass. The identity of the dark matter will still require some additional data, because moduli are not the only dark matter particles capable of producing an x-ray line. For example, sterile neutrinos, which can also be dark matter [13–16,38], are also expected to produce a line from their decay. Therefore, a discovery of an x-ray line from sources correlated with the dark matter

distribution would reveal the mass of the dark matter particle, but not necessarily its identity.

In this section we will assume that moduli make up 100% of dark matter. If dark matter comprises two or more components, and moduli make up fraction $f < 1$, the constraints derived for the decay width Γ_ϕ should be applied instead to the product $(f \times \Gamma_\phi)$, and those on b to $(f^{1/2} \times b)$.

A. X-ray data used for this study

As a proof of concept, we derive limits on the moduli decay rate in the soft x-ray energy band ($\sim$ 0.7–10 keV), based on observations of the Ursa Minor and Draco dwarf spheroidal galaxies conducted using the Suzaku X-ray Observatory. These data were obtained as part of a search for dark matter in the form of sterile neutrinos [39–41]. The advantage of using Suzaku data, as detailed in Ref. [39], lies in the low and stable internal background of the Suzaku XIS (X-ray Imaging Spectrometer) CCD detectors that, in combination with its sharp (by X-ray CCD standards) energy resolution, provides a robust and relatively sensitive capability for detecting faint spectral features over a broad (soft x-ray) bandpass. The motivation for targeting dwarf spheroidal galaxies is based on their proximity, high dark matter density, and absence of competing x-ray sources [39,40]. The Ursa Minor and Draco systems, which have among the highest known dark matter surface densities [42], remain the only dwarf spheroidals observed by Suzaku to date.

Utilizing these data, we derive limits on $\tau_{\phi\to\gamma\gamma}$, and hence on the moduli b parameter, for m_ϕ in the 1.5–20 keV mass range, as we now discuss in detail.

B. Data reduction, spectral analysis, and line flux limits

Spectral analysis of the Suzaku XIS data for Ursa Minor and Draco were previously presented in Refs. [39,40]. Given subsequent significant enhancements in calibration data, and in reduction and analysis tools, we reprocess and reanalyze the data as follows and also consider the data sets jointly for the first time.

Our reprocessing proceeds along standard lines[2] and follows that presented in Ref. [39], and more recently in Ref. [43], utilizing the Suzaku AEPIPELINE (version 1.0.1) ftool task. Details may be found in those papers (and references therein). Spectra are extracted from the entire fields of view for the back-illuminated (BI: XIS1) and two operational front-illuminated (FI: XIS0 and XIS3) chips, except for 4′-radius circular regions around the brightest point source in each XIS field of view, and 2′-radius circular regions around two fainter sources in the Draco field. Spectral redistribution matrix files (rmf) are generated using XISRMFGEN version 2011-07-02, effective area function files (arf) using XISSIMARFGEN version 2010-11-05. Spectra from the two FI detectors (XIS03 ≡ XIS0 + XIS3) are co-added and a weighted XIS03 response function calculated from their respective rmf and arf files. Finally, non-x-ray particle background (NXB) spectra are extracted from the appropriately selected and weighted night earth data using XISNXBGEN version 2010-08-22. All spectral fitting is conducted using XSPEC version 12.7.[3] Final good exposure times and total (including NXB) and "source" (NXB-subtracted) counts are displayed in Table I.

TABLE I. Exposures Times (in ks) and 0.6–7 keV Counts.

Galaxy	Detector	Time	Total	Source
UMinor	XIS03	138.1	10264	5745
UMinor	XIS1	69.05	8949	4380
Draco	XIS03	124.8	10361	6396
Draco	XIS1	62.4	9173	4636

We adopt two approaches for establishing baseline models via spectral fitting. In the first the NXB is subtracted, spectra in the 0.6–7 keV bandpass are grouped into bins with a minimum of 15 cts, and best-fit models are found by minimizing the χ^2 statistic. The models represent the astrophysical background and are composed of cosmic x-ray background and galactic x-ray background (GXB) components. The former is characterized as a power law, the latter as a soft thermal plasma. For Draco a two-temperature GXB model was required. Fits are performed jointly for Ursa Minor and Draco (but separately for XIS03 and XIS1). However, only the cosmic x-ray background slope is assumed identical in the two fields; GXB temperatures and all normalizations (expressed in units per solid angle) are untied. Reduced χ^2 in the best fit models are 0.97 (1038 degrees of freedom) for the XIS03 and 1.02 (918 degrees of freedom) for the XIS1 fits. These spectra, best-fit models, and residuals are shown in Fig. 1.

In the second approach, we consider the unsubtracted (total), unbinned spectra divided into four segments chosen to separate regions with and without strong NXB features. Overall, the spectra span the 0.7–10.5 (XIS03) and 0.7–7 (XIS1) keV energy ranges. Best-fit models are found by minimizing the modification of the C-statistic [44] implemented in XSPEC. In addition to the astrophysical background components detailed above, additional NXB power-law and emission line components are independently included in the models in each segment; see Ref. [39] for details. The results of these fits are shown in Fig. 2.

Once these baseline models are established, we add an unresolved Gaussian emission line, stepped through the full bandpass in 25 eV steps, and derive 99% upper

[2]see http://heasarc.gsfc.nasa.gov/docs/suzaku/analysis/abc/.

[3]http://heasarc.gsfc.nasa.gov/docs/xanadu/xspec/.

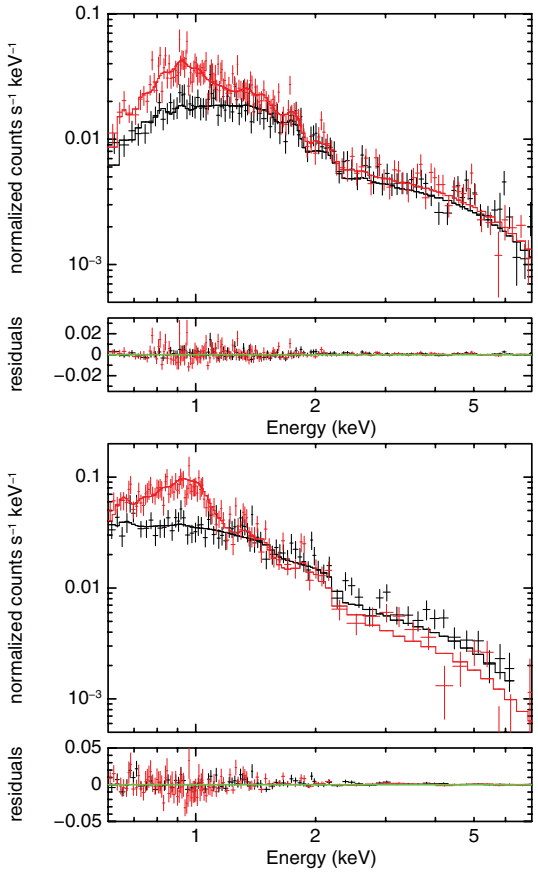

FIG. 1 (color online). 0.6–7 keV NXB-subtracted Suzaku XIS03 [top panel, (a)] and XIS1 [bottom panel, (b)] spectra of the Ursa Minor (black) and Draco (red) dwarf spheroidal galaxies (Draco has the greater low energy flux). The best joint-fit astrophysical background baseline models and residuals (data-minus-model) are also shown.

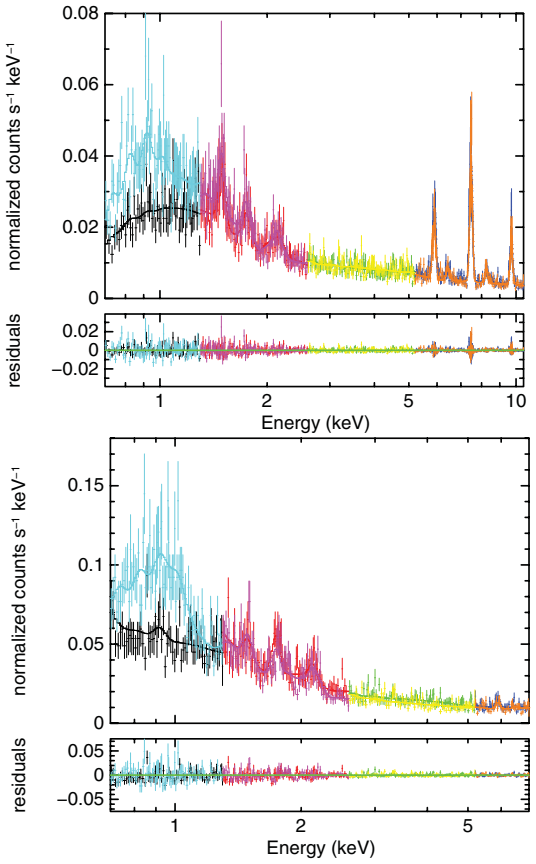

FIG. 2 (color online). Unsubtracted Suzaku XIS03 [top panel, (a)] and XIS1 [bottom panel, (b)] spectra of the Ursa Minor and Draco dwarf spheroidal galaxies (Draco has the greater low energy flux). The best joint-fit baseline models, that include both non-x-ray and astrophysical background components and residuals are also shown. The spectra are divided into segments spanning the following energies: 0.7–1.3 keV (Ursa Minor: black, Draco: light blue), 1.3–2.6 keV (Ursa Minor: red, Draco: magenta), 2.6–5.2 keV (Ursa Minor: green, Draco: yellow), 5.2–10.5 keV for XIS03 or 5.2–7 for XIS1 (Ursa Minor: blue, Draco: orange).

confidence levels (no significant detection was made) on the line surface brightness (that is permitted to be negative). The joint fits are conducted such that the three parameters of interest, in addition to the line energy, are the sum of the Draco and Ursa Minor line surface brightnesses and their ratio. Hence the 99% upper confidence level corresponds to Δ-statistic $= 11.3$.

C. Dark matter surface densities

Figure 3 shows the dynamically estimated mass profiles from Refs. [42,45], along with other determinations in the literature compiled by the latter. The Draco and Ursa Minor profiles are very similar within 600 pc, consistent with an NFW [46] profile with $M_{200} = 3\text{–}30 \times 10^9\ M_\odot$,[4] and a scale radius determined by the WMAP5 mass-concentration relation [47]. Within apertures of 7.7′—the region from which most of the source flux originates—and for distances of 77 (Ursa Minor) and 76 (Draco) kpc [42], the corresponding dark matter surface density for a (tidal) truncation radius of 1.5 kpc [48] is $\sim 150 \pm 50\ M_\odot\,\mathrm{pc}^{-2}$ for each galaxy, where the cutoff is implemented using the "$n = 2$ BMO" generalization of the NFW profile [49]. Including an additional summed Milky Way contribution of $\sim 150\ M_\odot\,\mathrm{pc}^{-2}$ [50], we adopt a fiducial summed, total line-of-sight surface mass density $\Sigma_{\mathrm{dm}} = 450\ M_\odot\,\mathrm{pc}^{-2}$, mindful that there is an uncertainty of at least $100\ M_\odot\,\mathrm{pc}^{-2}$.

D. Constraints on moduli dark matter

For our estimated summed dark matter surface mass density $\Sigma_{\mathrm{dm}} = 450\ M_\odot\,\mathrm{pc}^{-2}$, our 99% upper confidence levels on emission line surface brightness yield upper limits on the dark matter radiative decay rate over the Suzaku energy bandpass. We compare these limits as a

[4] where M_{200} is the mass encompassing an overdensity, relative to the critical density, of 200

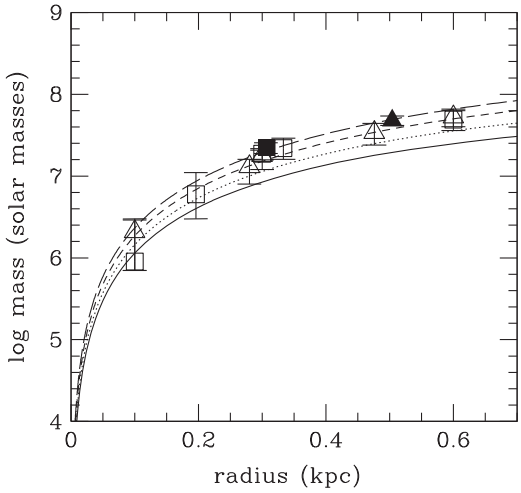

FIG. 3. NFW mass profiles for $M_{200} = 0.1$, 0.3, 1.0, and 3.0×10^{10} $M_\odot$ (solid, dotted, short-dashed, long-dashed curves, respectively) compared with estimates inferred by Ref. [42] (filled symbols) and inferred or compiled by Ref. [45] (open symbols); triangles (squares) denote Ursa Minor (Draco).

function of energy (in 150 eV bins) for the joint XIS03 analysis with the predicted decay rate of moduli dark matter for $b = 10$ [Eq. (3)] in Fig. 4. Our upper limits on b as a function of m_ϕ are shown in Fig. 5 for separate emission line limits from the XIS03 and XIS1 joint spectral analysis. Significant constraints on the moduli dark matter candidate are obtained in the ~8–20 keV mass range from this initial investigation. Significant improvements in sensitivity and mass range will be realized in observations made with the

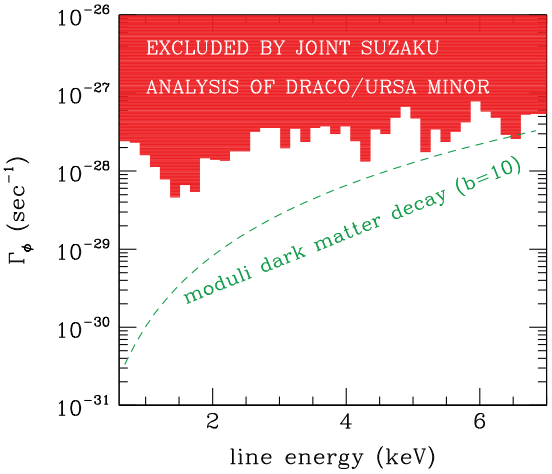

FIG. 4 (color online). Comparison of excluded dark matter radiative decay rate (shaded histogram) and predictions for moduli decay assuming $b = 10$. The limits are based on 99% upper confidence levels on line fluxes from joint analysis of Ursa Minor and Draco Suzaku XIS03 spectra and a summed, line-of-sight dark matter surface mass density $\Sigma_{dm} = 450$ $M_\odot$ pc^{-2}. In the case of a multicomponent dark matter, of which moduli make up fraction $f < 1$, the same constraints apply to the product $(f \times \Gamma_\phi)$.

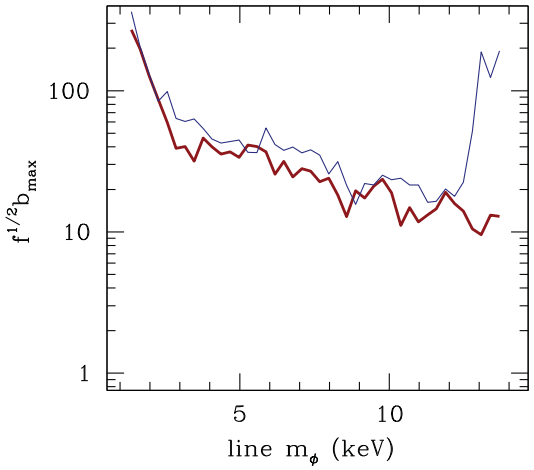

FIG. 5 (color online). Upper limit on the moduli b parameter representing the (inverse of) the effective moduli scale in units of the reduced Planck scale, based on 99% upper confidence levels on line fluxes from joint analysis of Ursa Minor and Draco Suzaku XIS03 (thick red line) and XIS1 (thin blue line) spectra and a summed dark matter surface mass density $\Sigma_{dm} = 450$ $M_\odot$ pc^{-2}. In the case of additional dark matter components that make up $(1 - f)$ of the total dark matter, the limit is on the product $(f^{1/2} \times b)$.

Astro-H Observatory,[5] scheduled for launch in 2014, with its capabilities for high energy resolution imaging spectroscopy in soft x rays (Soft X-ray Spectrometer) and low background, moderate energy resolution, imaging spectroscopy in hard x rays (Hard X-ray Imager).

VI. CONCLUSIONS

String moduli and supersymmetry moduli produced in the early Universe may exist as a form of dark matter. Current knowledge of supersymmetry breaking and the recent discovery of the 125 GeV Higgs boson imply that the masses of moduli particles are above about a keV, and the most interesting range is between 1 and 100 keV. In this range, x-ray telescopes may be able to detect a line from decay of these relic dark-matter particles. If such a line is detected, the photon energy will provide information about the particle mass.

We have presented the results of a search for such dark matter particles using the data from the first deep x-ray observations of the Draco and Ursa Minor dwarf spheroidal galaxies, dark-matter-dominated systems with extreme mass-to-light ratios and low intrinsic backgrounds. The absence of an emission line results in new constraints on the relevant new physics. The limits thus obtained are sufficiently interesting so as to raise the prospect of a search with improved range and sensitivity—and possibly a detection—in the near future, utilizing expected upgrades in the capabilities of x-ray observatories.

[5]http://heasarc.gsfc.nasa.gov/docs/astroh/.

ACKNOWLEDGMENTS

The work of A. K. was supported by the DOE Grant No. DE-FG03-91ER40662. A. K. appreciates the hospitality of the Aspen Center for Physics, which is supported by the NSF Grant No. PHY-1066293. M. L. was supported by NASA ADAP Grants No. NNX11AD36G and No. NNX11AD11G and the Astro-H mission.

[1] E. Witten, Nucl. Phys. **B471**, 135 (1996).
[2] P. Svrcek and E. Witten, J. High Energy Phys. 06 (2006) 051.
[3] ATLAS Collaboration, Phys. Lett. B **716**, 1 (2012).
[4] CMS Collaboration, Phys. Lett. B **716**, 30 (2012).
[5] Y. Okada, M. Yamaguchi, and T. Yanagida, Phys. Lett. B **262**, 54 (1991).
[6] M. Ibe, S. Matsumoto, and T. T. Yanagida, Phys. Rev. D **85**, 095011 (2012).
[7] N. Arkani-Hamed, J. March-Russell and H. Murayama, Nucl. Phys. **B509**, 3 (1998).
[8] M. Fujii and T. Yanagida, Phys. Lett. B **549**, 273 (2002).
[9] E. A. Baltz and H. Murayama, J. High Energy Phys. 05 (2003) 067.
[10] K. Petraki, Phys. Rev. D **77**, 105004 (2008).
[11] D. Boyanovsky, Phys. Rev. D **78**, 103505 (2008).
[12] D. Boyanovsky, Phys. Rev. D **77**, 023528 (2008).
[13] T. Asaka, M. Shaposhnikov, and A. Kusenko, Phys. Lett. B **638**, 401 (2006).
[14] A. Kusenko, Phys. Rev. Lett. **97**, 241301 (2006).
[15] K. Petraki and A. Kusenko, Phys. Rev. D **77**, 065014 (2008).
[16] A. Kusenko, F. Takahashi, and T. T. Yanagida, Phys. Lett. B **693**, 144 (2010).
[17] E. Dudas and C. Grojean, Nucl. Phys. **B507**, 553 (1997).
[18] M. Dine, W. Fischler, and D. Nemeschansky, Phys. Lett. **136B**, 169 (1984); O. Bertolami and G. G. Ross, Phys. Lett. B **183**, 163 (1987); M. Dine, L. Randall, and S. D. Thomas, Phys. Rev. Lett. **75**, 398 (1995); A. Kusenko, Phys. Lett. B **377**, 245 (1996).
[19] G. R. Dvali, Phys. Lett. B **355**, 78 (1995).
[20] I. Affleck and M. Dine, Nucl. Phys. **B249**, 361 (1985).
[21] T. Moroi, M. Yamaguchi, and T. Yanagida, Phys. Lett. B **342**, 105 (1995).
[22] M. Dine and A. Kusenko, Rev. Mod. Phys. **76**, 1 (2003).
[23] G. M. Fuller, C. T. Kishimoto, and A. Kusenko, arXiv:1110.6479.
[24] J. L. Menestrina and R. J. Scherrer, Phys. Rev. D **85**, 047301 (2012).
[25] J. Hashiba, M. Kawasaki, and T. Yanagida, Phys. Rev. Lett. **79**, 4525 (1997).
[26] T. Asaka, J. Hashiba, M. Kawasaki, and T. Yanagida, Phys. Rev. D **58**, 083509 (1998).
[27] T. Asaka, J. Hashiba, M. Kawasaki, and T. Yanagida, Phys. Rev. D **58**, 023507 (1998).
[28] S. Kasuya, M. Kawasaki, and F. Takahashi, Phys. Rev. D **65**, 063509 (2002).
[29] D. H. Lyth and E. D. Stewart, Phys. Rev. Lett. **75**, 201 (1995).
[30] D. H. Lyth and E. D. Stewart, Phys. Rev. D **53**, 1784 (1996).
[31] A. D. Linde, Phys. Rev. D **53**, R4129 (1996).
[32] K. Nakayama, F. Takahashi, and T. T. Yanagida, Phys. Rev. D **84**, 123523 (2011).
[33] M. Tegmark, A. Aguirre, M. Rees, and F. Wilczek, Phys. Rev. D **73**, 023505 (2006).
[34] A. D. Linde, Phys. Lett. B **259**, 38 (1991).
[35] M. Tegmark and M. J. Rees, Astrophys. J. **499**, 526 (1998).
[36] L. Zhang, X. Chen, M. Kamionkowski, Z. g. Si and Z. Zheng, Phys. Rev. D **76**, 061301 (2007).
[37] S. De Lope Amigo, W. Y. Cheung, Z. Huang, and S. P. Ng, J. Cosmol. Astropart. Phys. 06 (2009) 005.
[38] S. Dodelson and L. M. Widrow, Phys. Rev. Lett. **72**, 17 (1994); K. Abazajian, G. M. Fuller, and M. Patel, Phys. Rev. D **64**, 023501 (2001); K. Abazajian, G. M. Fuller, and W. H. Tucker, Astrophys. J. **562**, 593 (2001); A. D. Dolgov and S. H. Hansen, Astropart. Phys. **16**, 339 (2002); T. Asaka, S. Blanchet, and M. Shaposhnikov, Phys. Lett. B **631**, 151 (2005); A. Boyarsky, O. Ruchayskiy, and M. Shaposhnikov, Annu. Rev. Nucl. Part. Sci. **59**, 191 (2009); A. Kusenko, Phys. Rep. **481**, 1 (2009).
[39] M. Loewenstein, A. Kusenko, and P. L. Biermann, Astrophys. J. **700**, 426 (2009).
[40] M. Loewenstein and A. Kusenko, Astrophys. J. **714**, 652 (2010).
[41] M. Loewenstein and A. Kusenko, Astrophys. J. **751**, 82 (2012).
[42] J. Wolf, G. D. Martinez, J. S. Bullock, M. Kaplinghat, M. Geha, R. R. Muñoz, J. D. Simon, and F. F. Avedo, Mon. Not. R. Astron. Soc. **406**, 1220 (2010).
[43] M. Loewenstein and D. Davis, Astrophys. J. **757**, 121 (2012).
[44] W. Cash, Astrophys. J. **228**, 939 (1979).
[45] N. C. Amorisco and N. W. Evans, Mon. Not. R. Astron. Soc. **411**, 2118 (2011).
[46] J. F. Navarro, C. S. Frenk, and S. D. M. White, Astrophys. J. **490**, 493 (1997).
[47] A. V. Macciò, A. A. Dutton and F. C. Van Den Bosch, Mon. Not. R. Astron. Soc. **391**, 1940 (2008).
[48] M. A. Sanchez-Conde, M. Cannoni, F. Zandanel, M. E. Gomez, and F. Prada, J. Cosmol. Astropart. Phys. 12 (2011) 011.
[49] M. Oguri and T. Hamana, Mon. Not. R. Astron. Soc. **414**, 1851 (2011).
[50] E. Borriello, M. Paolillo, G. Miele, G. Longo, and R. Owen, Mon. Not. R. Astron. Soc. **425**, 1628 (2012).